

Final Report

Plasma-Activated Irrigation for Improving Soybean Development and Disease Tolerance

Dr. Sungo Kim (PI), Department of Electrical and Computer Engineering, College of Engineering, Kansas State University, Phone: 785-532-5678, Email: sungo@ksu.edu.

Dr. Chris Little (Co-PI), Department of Plant Pathology, Kansas State University, Phone: 785-532-1395, Email: clittle@ksu.edu.

1. Remained Research Objectives

We still need to conduct experiments about the attached objectives to achieve good research results so that we can verify a relationship and effect between plasma and soybean plants. I attached the remaining parts of the objectives.

Flexible plasma bundle devices: Highly flexible plasma bundle devices using optical fibers, which can generate cold plasma and be inserted into a water reservoir without any contact of plasma electronics, will be fabricated. The PI has recently discovered the novel plasma jet-to-jet coupling effect that can generate strong plasma energy. **Plasma-activated water:** Plasma generates OH radicals in water using a plasma bundle device so that plasma-activated water sterilizes and refresh soil and soybean plants. When microorganisms are treated with plasma and die due to loss of hydrogen atoms in the cell membranes which become water molecules. (2) *Measuring growth rate and yield components (Obj. 1)*. Soybeans will be planted in large pots in an RCBD under carefully controlled conditions in the greenhouse. Pot water holding capacity will be adjusted to field capacity prior to planting and maintained at this level throughout host development using either regular water or plasma-activated irrigation. Seed emergence and vigor will be measured from VE to V3. Time between vegetative development stages, time to flowering, and pod development will be measured in adult plants. Number of flowers, pods, and seeds per pod will be counted and compared between treatments to estimate yield components. (3) *Measuring soybean sudden death and charcoal rot disease symptoms (Obj. 2)*. In another experiment, plants will be artificially inoculated with *Fusarium virguliforme* (SDS), *M. phaseolina* (charcoal rot), or mock-inoculated (control). The experiment will be conducted in the growth chamber. In the case of SDS, seeds will be planted in a matrix of pre-colonized pathogen inoculum and allowed to germinate and develop roots. SDS symptoms will be rated at the V3-V4 seedling stage using a 0 to 9 scale based on the degree of foliar chlorosis and necrosis. For charcoal rot, plants will be established in larger pots in a similar pathogen-colonized matrix to allow for root infection. A period of temperature stress (35°C for 7 days) will be induced prior to flowering to encourage disease development. Plants will be rated for wilting symptoms and roots will be harvested and assessed for pathogen colony-forming units to see if host colonization differs between treatments. For both diseases, individual pots will be irrigated to field capacity (as in #2 above) with either regular water or plasma-activated water. As in #2, experiments will be set up using an RCBD.

2. Current Statement

We fabricated a single glass tube based atmospheric pressure plasma device to treat soybean seeds treatment. And we characterized basic I-V characteristics and optical emission spectra as below. I attached the summary from the progress report of work 3.

The schematic diagram of experimental set-up for seed germination is shown in Figure 1. We prepared for 25 petri dishes and each dish has 10 seeds. We treated seeds by direct plasma for 30 seconds, 1 min, 3 min, and 5 min. And we also treated seeds by plasma activated water which is treated by plasma for 30 min and 1 hour. We will compare growth rate and yield in controls, directed plasma treated seeds, and plasma activated water treated seeds (indirect plasma treated seeds).

Figure 2 shows the plasma treatment for seeds germination. The glass tube employed had an inner diameter of 1mm and an outer diameter of 2 mm. The plasma plume from this microplasma jet device would be able to precisely treat soybean seeds. Copper tape, 6 mm wide, was used as a single electrode that was placed 5 mm from the end of the glass tube. High purity helium gas was used as the discharge gas. The helium gas flow rate was held constant at approximately 35 standard cubic centimeters per minute (sccm). To determine the input electric energy, the voltage and current waveforms emanating from the powered electrode were measured using a high voltage probe (Tektronix P6015A) and a current monitor (Pearson 4100). An inverter circuit was used to amplify a low primary voltage to a high secondary voltage. The driving circuit generates a sinusoidal voltage of several tens kilovolts with a frequency of several tens of kilohertz. The photosensor amplifier (Hamamatsu C6386-01) was used to observe the plasma emission. The wavelength unresolved optical emission waveform from the photosensor amplifier that covered the wavelength ranges of 400–1100 nm was plotted on the digital oscilloscope (Tektronix TDS3014C). In the front of the photo sensor amplifier, the optical slit 1 mm wide is used to avoid unwanted light signals from the environment. The fiber optic spectrometer (Ocean Optics USB-4000UV-VIS) was used to identify the various reactive species and observe the change of the emitting spectra of reactive species with a change of experimental condition. To verify the general electrical and optical properties of this plasma jet, the discharge current and optical emissions were measured as a function of time as shown in Fig. 3. All data were averaged over 16 waveform periods for reliable averaging. The discharge current was obtained by subtracting the displacement current from the total current plotted on the digital oscilloscope. The discharge current waveform shows that the discharge occurred not only in the rising periods but also in the falling periods of the voltage waveforms. While discharges occurred more than twice in the rising periods of the voltage waveforms, however, they occurred once in the falling period.

Figure 3 also shows the temporal intensity of optical emissions from the plasma jets in the ambient air, which is measured at 5 mm from the end of the theta tube. The optical intensity is much higher during the increasing of the voltage waveform than during the decreasing of the voltage waveform. Note that the time points of the discharges observed by the discharge current and the optical emission intensity are the same. The discharge current and the optical emission intensity indicate that stronger plasmas are generated when the single electrode is used as the anode. Nonetheless, this plasma jets are very stable because the discharge currents and the optical emission intensities have periodically equivalent shape and timing during the discharge processes. It also shows that every discharge occurs within the rising and falling periods of the voltage waveforms, respectively, indicating that the discharges were well produced even if the single

electrode plays a role of both an anode and a cathode. To identify the diverse reactive species generated by the plasma in the ambient air and verify the increase of oxygen in the plasma, the emission spectra of the atmospheric pressure plasma jet were monitored using a fiber optic spectrometer.

As shown in Fig. 4a, the emission spectra verified the presence of excited N_2 , N_2^+ , He, and O species in the plasma plumes produced by helium gas without oxygen flow over the spectral range from 270 to 850 nm. Fig. 4b provides the emission spectra of helium plasma with oxygen flow of 100 sccm, which exhibits increased oxygen and decreased nitrogen compared with the data of Fig. 4a. To investigate the dependence of oxygen gas flow rate in greater detail, the O₂ flow rate was gradually increased from 0 to 100 sccm (0, 5, 10, 30, 50, and 100 sccm) in one of the hollow channels of the theta tube under identical input voltage (peak voltage of 7.5 kV with 32 kHz) and helium flow rate of 100 sccm. As a result, the oxygen peaks of 777.1 nm and 844.6 nm increase with increasing O₂ flow rate, as shown in the magnified emission spectra of Fig. 4c and 4d. Even if the oxygen plasma is not produced in air, O₂ surely participates in the plasma process and affects the plasma properties. This amplitude change of the oxygen peaks is a strong evidence that we can control the ROS in plasma medium as a change of O₂ flow rate without additional voltage applying. Interestingly, when the oxygen flow rate is gradually increased, the second positive systems of nitrogen, nitrogen peaks of 315.9 nm and 337.1 nm, are gradually decreased as shown in Fig. 4e and 4f. This is likely due to the increase in oxygen concentration in the air near the plasma device. If the oxygen contents increased in the air near the plasma device, the nitrogen content in the air should relatively decrease such that the nitrogen peaks also are decreased. The results indeed show that even without an oxygen plasma jet in the air, the oxygen flow contributes to the plasma process and sufficiently affects the plasma characteristics. In addition, the proposed device provides a unique advantage to control amount of ROS with precise change of oxygen gas flow rate. We need to conduct experiments for seed germination for making growth rate and yield data with petri dishes as shown in figure 1.

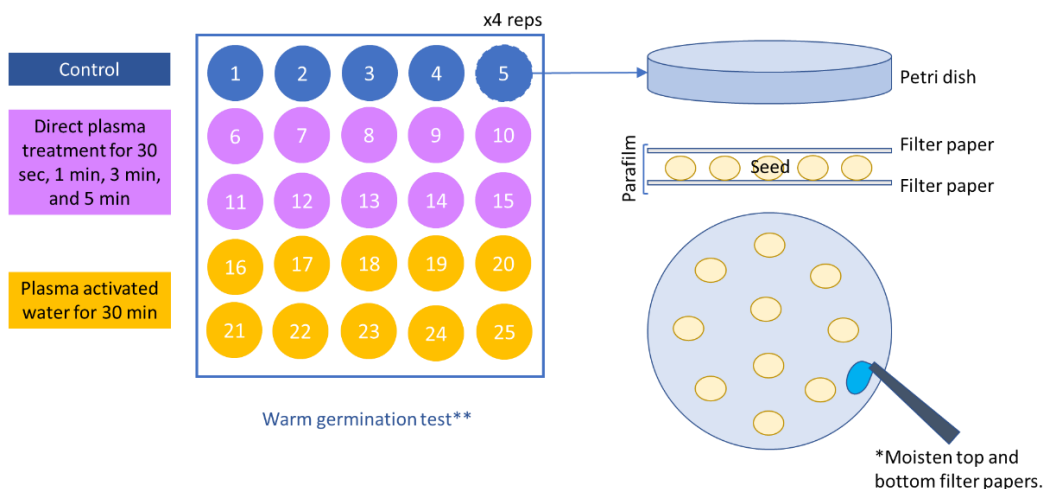


Figure 1. Schematic diagram of experimental set-up for plasma treatment.



Figure 2. Direct plasma treatment for seed germination.

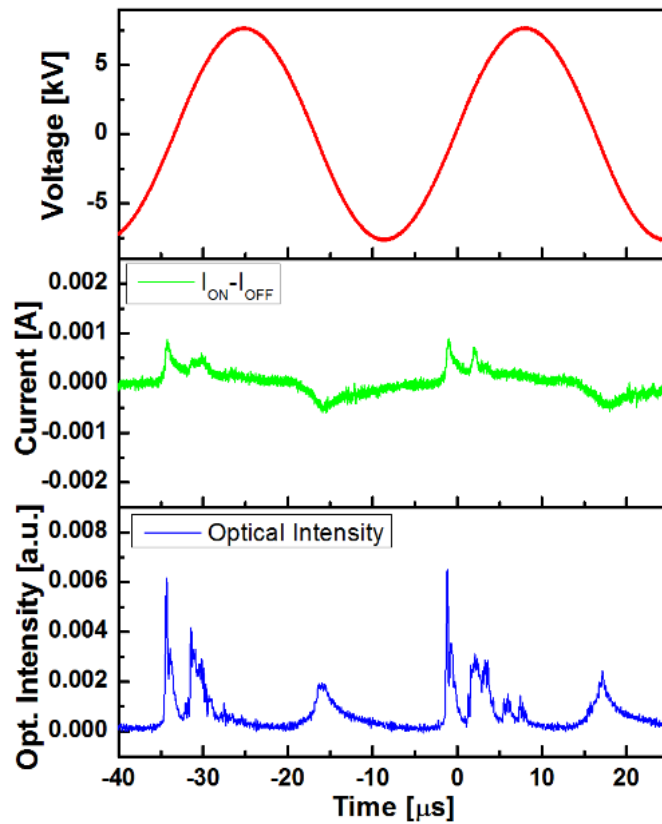


Figure 3. Temporal distribution of discharge current, obtained by subtracting displacement current from total current discharge waveform, and optical emission intensity from the plasma jets, which is measured 5 mm away from device nozzle.

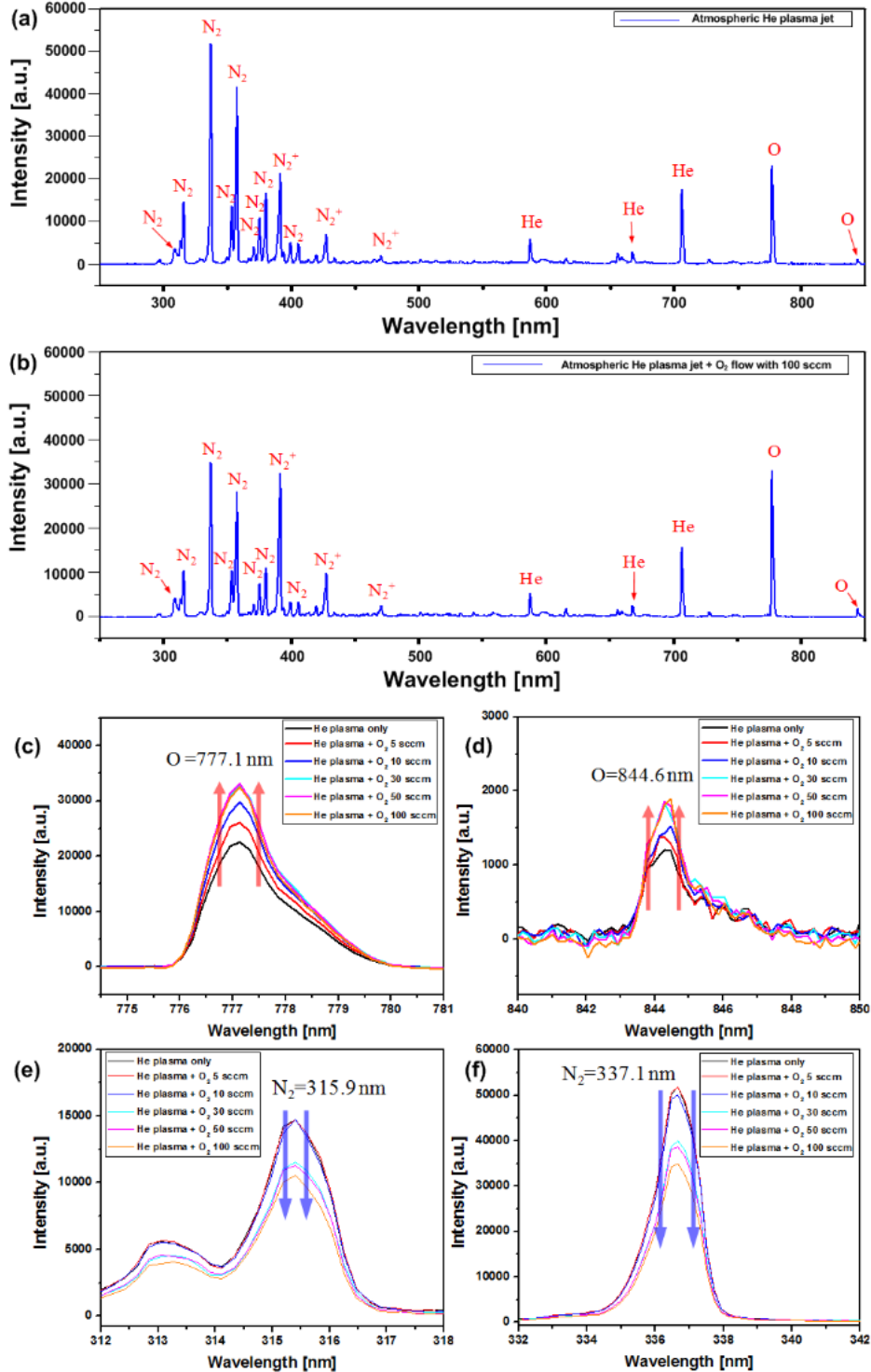


Figure 4. Optical emission spectra (OES) of atmospheric pressure helium plasma plumes (a) without oxygen flow and (b) with oxygen flow of 100 sccm over the range from 270 to 850 nm. Changes in emission spectra of oxygen peaks of (c) 777.1 nm and (d) 844.6 nm with an increase of oxygen gas flow rate, respectively. Changes in emission spectra of nitrogen peaks of (e) 315.9 nm and (f) 337.1 nm with an increase of oxygen gas flow rate, respectively.

3. Research Plan

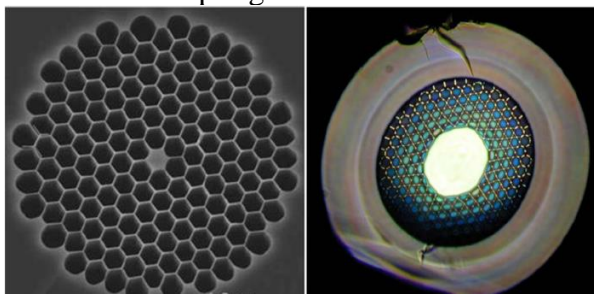
Our research team currently cannot conduct advanced experiments to characterize plasma properties so that we can recognize which plasma species are dominant factors for growth rate, yield, and disease resistance. We need to fabricate proposed optical fibers to use jet-to-jet coupling for accelerating plasma effect for soybean plants. We need high-power generators to make a plasma activated water. We also need to purchase plasma measurement instruments such as high voltage probe, photosensor amplifiers, ICCD camera, optical emission spectroscopy, software, and materials and supplies. Unfortunately, we cannot proceed our experiments because the fund has been blocked. Please allow us the fund to use so that we can conduct the proposed experiments.

Develop high performance, intense and high-density atmospheric pressure micro-plasma jets

Method 1: Various shaped atmospheric plasma jet arrays for intense and high-density plasma jet

We will fabricate honeycomb structured atmospheric pressure plasma jet arrays with 7 and 19 quartz/glass tubes, and multi-layered PCFs to make the intense and high-density plasma. We will also fabricate multi-layered PCFs using a custom-designed commercial-scale Heathway optical fiber draw tower. The PCFs have exceedingly strong, long and inexpensive fibers (> km) due to the maturity of the optical fiber fabrication process. **Fig 5** shows the proposed multi-layered PCFs. The proposed PCF based intense and high-density micro-plasma jets have advantages in flexibility, micro-scale, and multi-layered and stronger coupling effect. We also will fabricate PCFs with internal electrodes with the advantages of packaging, flexibility, energy conversion (high energy efficiency), and applications.

Figure 5. Proposed multi-layered PCFs to enforce the coupling effect.



Method 2: Various gas flow rates and gases/gas mixtures for easy jet-to-jet coupling and high-energetic plasma to increase treatment effect

We determined that the gas velocity (gas flow rate) is one of the key parameters for producing intense plasma mode as well as distance between the device and ITO-coated glass, and dependence of the dielectric constant by the thickness of ITO-coated glass. Each element tube has an identical gas flow rate in the existing plasma devices. We will differentiate the gas flow rates between centered tube and outer tubes to determine the coupling degrees for fine and strong jet-to-jet coupling. We will also apply various gases and gas mixtures to plasma devices (e.g. argon, argon balanced oxygen, and helium balanced oxygen) to understand these optimal coupling conditions.

Method 3: Dependence of input voltage waveform and driving frequency

The driving conditions (voltage waveform and driving frequency) are a necessary prerequisite for developing the fine intense plasma at atmospheric pressures. For example, when the driving frequency doubles in low-frequency and high voltage plasma conditions (ex. 25 kHz → 50 kHz), the discharges occur twice as often previous discharges of the same duration, resulting

in intense and high-density plasmas. We will apply various voltage waveforms (sinusoidal, square pulse, and impulse waveforms) with various driving frequencies to cold plasma devices and investigate the correlation between the jet-to-jet coupling and driving conditions.

Directly characterize jet-to-jet coupling in plasma arrays and plasma-to-materials interactions from nano- to many seconds after ignition, and dependence on various conditions

Method 1: Spatial and temporal coupling behaviors of plasma bullet

Intensified CCD measurements involve using the shutter and gate modes to image time-averaged visible-infrared emissions and the temporal behavior of VIS/IR emissions respectively. The shutter mode of the ICCD camera will provide valuable information on the intensity of VIS/IR emissions from our devices. We will investigate the spatial distribution of reactive species using the shutter mode of the ICCD images. The gate mode of the ICCD camera will provide the time of resolved behavior of the VIS/IR emission from the plasma within the tubes and between the tubes and the ground electrode. Using the gate mode of the ICCD camera, we will observe the temporal coupling behaviors of plasma bullet from our devices. Besides, we can calculate the velocity of the plasma bullet using the gate mode.

Method 2: Temporal delay during plasma processes including direct plasma jet-to-jet coupling

When the plasma jets merge at the orifice of the array device in the intense plasma mode, the spatial and temporal interacted behavior can be observed using the gate mode of the ICCD camera. We will investigate this spatial and temporal interaction among the plasma plumes in detail to explain the mechanism of direct plasma jet-to-jet coupling. The spatial and temporal interaction is expected to lead to the discharge delay. We will check the discharge delay observation by ICCD images to the experimental results using photo sensor amplifier.

Method 3: Modeling by simulation and experiment for jet-to-jet coupling and plasma-to-materials interactions

We will determine a numerical analysis of our findings for comparison with our experimental results. The ion and electron temperature/density, electric field distribution, relationship between/among plasmas and materials will be compared by both simulation and experiment. This study will provide the further understanding of jet-to-jet coupling in the proposed atmospheric pressure plasma arrays.

Measure electron energy/density, density of charged particles, and plasma temperature during plasma processes to define intense and high-density atmospheric pressure plasma

Method 1: Discharge status of plasma devices

We will determine the discharge status, the success or failure by the visible and infrared emission waveform from the photo sensor amplifier. The photo sensor amplifier permits measured discharge information as a function of time such as ignition time of plasmas, discharge delay, and discharge duration time. The VIS/IR emission waveform from photo sensor amplifier also shows the plasma stability by indicating the periodicity and consistency of discharge as a function of time. This observation method will provide valuable information on the intensity and duration of plasma emission in our plasma devices.

Method 2: Electrical breakdown and I-V characteristics of plasma devices

As most cold atmospheric pressure plasma devices driven by voltage control, obtaining voltage levels and waveforms are essential for determining electrical characteristics. Moreover, the voltage difference between initial and sustaining discharge indicates an accumulated charge on the dielectric layer that is integral in controlling discharge currents by internal fields, thusly preventing glow to the arc transition. I-V characteristics can also provide power consumption of plasma devices. I-V measurements indirectly can help to estimate electron density, N_e and electron temperature, T_e by calculation of the reduced electric field (electric field divided by gas density) E/N .

Method 3: Electron energy/density by optical emission spectroscopy-based techniques

Optical emission spectroscopy (OES) is a noninvasive probing method for investigating atoms, ions, and molecules in plasma. Its diagnostic use for emitting media has yielded a greater understanding of very complex phenomena such as high gas pressure plasmas. To determine the presence of high electron energy in our proposed intense plasma, we will characterize the properties of that energy using OES of the second positive systems of nitrogen. The nitrogen molecule is transferrable from the ground state $N_2(X^1\Sigma_g^+)$ into an excited state $N_2(C^3\Pi_u)$ by the impact of electrons with energy greater than 11.0 eV. Subsequently, the excited $N_2(C^3\Pi_u)$ molecules will transfer into the $N_2(B^3\Pi_g)$ state by emitting a photon of the 337.1 nm wavelength. If electrons exhibit energy greater than 18.7 eV, nitrogen ions $N_2^+(B^2\Sigma_u^+)$ will be produced that will release photons of 391.4 nm wavelength via transfer into the $N_2^+(X^2\Sigma_g^+)$ state. The relative changes in the concentration of active species $N_2(C^3\Pi_u)$ and $N_2^+(B^2\Sigma_u^+)$ in the intense and normal plasma plumes will be monitored by measuring the emission intensities at 391.4 nm and 337.1 nm. If the emission intensity at 391.4 nm is increased in the intense plasma mode, the electron energy of the intense plasma is revealed to be relatively larger than that of the normal plasma. The line ratio method using OES, in which the intensity ratio of emission lines is related to the electron density by a collisional–radiative model (CRM) has been successfully used in low- and medium-pressure discharges. We will first determine the CRMs of atmospheric pressure discharges with carrier gases (He or Ar) and then the electron density through an experimental line-ratio method.

Method 4: Investigation of various parameters of electron plasma component using BLOSIG+

Using the electron Boltzmann equation solver, BLOSIG+, we will identify the reactive species and investigate parameters of the electron plasma component that are expressed as a function of the reduced electric field, E/N , such as electron mobility, μ_e , drift velocity of electrons, V_{dr} , average electron energy, and reaction rate constant, K . We also expect to interpret the values of some parameters through matching with the calculated values from our experimental results.